Chemical Engineering Science 214 (2020) 115396

Contents lists available at ScienceDirect

Chemical Engineering Science

journal homepage: www.elsevier.com/locate/ces

Molecular dynamics simulations of the removal of lead(II) from water using the UiO-66 metal-organic framework

Malak Wehbe [a,1], Belal J. Abu Tarboush [a], Mutasem Shehadeh [b,*], Mohammad Ahmad [a]

[a] Bahaa and Walid Bassatne Department of Chemical Engineering and Advanced Energy, American University of Beirut, Beirut, Lebanon
[b] Mechanical Engineering Department, American University of Beirut, Beirut, Lebanon

HIGHLIGHTS

- Molecular dynamics simulations to study the UiO-66 MOF for removing Pb^{2+} ions from water.
- Optimal conditions for Pb^{2+} removal are: low number density of particles, high metal concentration and absence of NO_3^- ions.
- Strong intermolecular interaction between Pb^{2+} and NO_3^- ions leads to a significant reduction in Pb^{2+} removal.
- Electrostatic interaction between O atoms and Pb^{2+} is the proposed adsorption mechanism.

ARTICLE INFO

Article history:
Received 10 May 2019
Received in revised form 4 November 2019
Accepted 27 November 2019
Available online 29 November 2019

Keywords:
Molecular dynamics
Water treatment
Adsorption
Metal-organic framework
Lead(II)
UiO-66

ABSTRACT

In this work, we use molecular dynamics simulations to investigate the viability of using the UiO-66 MOF for the removal of lead ions, Pb^{2+}, from water. We study the concentration of Pb(II) in water in the presence of this MOF under varying conditions of number density of particles in the system (500, 300, 74 and 20 particles), metal cation concentration (1.5 M, 3.7 M, 6 M and 55.6 M) and presence of NO_3^- ions. Pb(II) ions are observed to adsorb onto the UiO-66 framework under favorable conditions, corresponding to: low number density of particles, high metal cation concentration and absence of NO_3^- ions in the vicinity of the MOF. According to the radial distribution functions, preferential adsorption sites for the Pb^{2+} in UiO-66 correspond to the oxygen atoms forming the Zr–O–Zr bridge. This study indicates that UiO-66 could be a successful candidate for the removal of Pb(II) from water.

1. Introduction

Heavy metals have gained increasing public and scientific attention in recent years due to their environmental contamination and the significant rise in human exposure (Bradl, 2005; Tchounwou et al., 2012). Lead is a heavy metal which is toxic to humans even at low levels of exposure (Duffus, 2002). Humans can be exposed to lead in various ways including: inhalation of lead-contaminated dust particles or ingestion of lead-contaminated food, water and paints (Tchounwou et al., 2012). However, drinking water is the main source for exposure. For example, in the USA, 35–50% of the Pb(II) absorbed by adults is through drinking water, and this proportion can be greater than 50% for children (Agency for Toxic Substances and Disease Registry, 2007; Tchounwou et al., 2012). While lead is naturally occurring, it is the anthropogenic activities, such as: burning fossil fuels, mining and manufacturing processes, that play a role in releasing high concentrations of the metal (Tchounwou et al., 2012). The presence of lead in drinking water is mostly due to the corrosion of plumbing material belonging to water systems (Environmental Protection Agency, 2019). In humans, lead poisoning directly affects the nervous system and all organs in the body, leading to anemia, renal dysfunction, heart disease and even death (Agency for Toxic Substances and Disease Registry, 2007; Flora et al., 2012; Harvey, 2002). Hence, the U.S. Environmental Protection Agency (U.S. EPA) (Environmental Protection Agency, 2019) and World Health Organization (WHO) (WHO, 2008) enforced maximum allowable concentrations of lead in drinking water of 0.015 mg/l and 0.01 mg/l, respectively. The toxic effects of Pb(II) and its inevitable presence in drinking water call for the development of effective techniques for its removal.

* Corresponding author.
E-mail address: ms144@aub.edu.lb (M. Shehadeh).
[1] Currently at the Department of Chemical Engineering, Centre for Process Systems Engineering, Imperial College London, South Kensington Campus, London SW7 2AZ, United Kingdom.

https://doi.org/10.1016/j.ces.2019.115396
0009-2509/

Various methods have been used for the removal of Pb(II) from drinking water including: adsorption, reverse osmosis, ion exchange, membrane filtration, cementation, chemical precipitation, coagulation and flocculation, flotation and electrochemical treatment (Fu and Wang, 2011; Ihsanullah et al., 2016). Adsorption is the most commonly used method, due to its low cost and flexible operation (Barakat, 2011; K. Wang et al., 2017). Among others, activated carbon adsorbents are commonly used for the removal of heavy metals from water but these are relatively expensive, have low adsorption capacities and lack functional tunability (Fu and Wang, 2011; K. Wang et al., 2017). There is significant interest in the development of more economic and effective adsorbents.

Metal-organic frameworks (MOFs) are organic-inorganic hybrid material that have emerged and attracted attention since the 1990s due to their high surface areas (up to 6500 m^2/g), wide range of pore sizes (up to 4.5 nm) and tunable functionality (Nalaparaju and Jiang, 2012; K. Wang et al., 2017; Zhou et al., 2012); making them versatile for diverse applications such as: gas storage (Burrows et al., 2008; Dietzel et al., 2008; Dincă and Long, 2008; C.-J. Li et al., 2008; K. Li et al., 2008; Murray et al., 2009), adsorption (Lin et al., 2016; Wang et al., 2015), ion exchange (Custelcean et al., 2007; Nalaparaju and Jiang, 2012), drug delivery (Horcajada et al., 2006), catalysis (Farrusseng et al., 2009; Lee et al., 2009) and sensing (Halder et al., 2002). Perhaps a challenge associated with using MOFs for water treatment is their water-stability, since the structure of most MOFs is disrupted in water. The presence of many oxygen-metal bonds can lead to the hydrolysis and irreversible loss of the framework (Cychosz and Matzger, 2010). An example of this is MOF-5 (Greathouse and Allendorf, 2006). However, several water-stable MOFs have been used for the removal of heavy metal ions from water (Barakat, 2011; Howarth et al., 2015; Jamali et al., 2016; Ke et al., 2011; Luo et al., 2015; Qin et al., 2011; Tahmasebi et al., 2015; Vu et al., 2015; L. Wang et al., 2017; Yee et al., 2013; Yin et al., 2016; Zhang et al., 2016; Zou et al., 2013). Specifically, amino-functionalized Cr-MOF (MIL-101) (Luo et al., 2015), azine-functionalized Zn-MOF (TMU-5) (Tahmasebi et al., 2015), zinc-based ZIF-8 (L. Wang et al., 2017), MnO_2-MOF (Qin et al., 2011), HKUST-1-MW@$H_3PW_{12}O_{40}$ (Zou et al., 2013), lanthanide-based Dy(BTC)(H_2O).$(DMF)_{1.1}$ (Jamali et al., 2016) and thiol-functionalized HS-mSi@MOF-5 (Zhang et al., 2016) have been used for the removal of Pb(II) from water, mainly via adsorption.

In recent years, zirconium-based MOFs have emerged as having exceptional thermal and water stabilities (Cavka et al., 2008; DeCoste et al., 2013; Liu et al., 2015). Particularly, UiO-66, composed of $Zr_6O_4(OH)_4$ clusters and terephthalate (1,4-benzenedicarboxylate, BDC) linkers, has been used repeatedly for water treatment (Hasan and Jhung, 2015; Howarth et al., 2015; Khan et al., 2015; Liu et al., 2015; Seo et al., 2015; Wang et al., 2015). Together with its stability, UiO-66 exhibits a highly porous structure and a Langmuir surface area of 1187 m^2/g, making it a suitable candidate for water treatment (Cavka et al., 2008; Yang et al., 2011). Despite this, very little work in literature has focused on the removal of heavy metals from water using UiO-66. To the best of our knowledge, only the work by Wang et al. (Wang et al., 2015) experimentally investigated the removal of arsenate, As(V), from water using this MOF. Chemical adsorption was the proposed mechanism, with an adsorption capacity of 303 mg/g at the optimal pH (Wang et al., 2015).

In this work, we present a molecular dynamics (MD) simulation study to investigate the removal of the toxic Pb(II) from water using the chemically stable UiO-66 MOF. To date, only few computational works have studied the removal of heavy metal ions from water using MOFs. Nalaparaju and Jiang (2012) used MD simulations to investigate the ion exchange process between non-framework Na^+ ions, in rho-ZMOF, and Pb^{2+} ions. All the Pb(II) ions resided in the MOF at equilibrium, completely exchanging the Na^+ ions, showing a good potential for this MOF in water purification. The nanoscopic analysis made possible by these MD simulations will lead to an accurate understanding of the viability of the removal of Pb(II) ions prior to running experiments. We study the concentration of Pb^{2+} ions in water in a system containing UiO-66. Due to the continuously changing conditions near the MOF in water, the effect of the cation/water mixture number density, metal cation concentration and presence of nitrate (NO_3^-) ions will be studied to identify the optimal conditions for removal. It should be noted that our simulations present conditions in a region *close* to the MOF and not those of the bulk phase. Therefore, the aim of our work is to study the *mechanism* by which metal uptake occurs (if any). Additionally, to gain an insight of the adsorption mechanism in the MOF, radial distribution functions (RDFs) of Pb^{2+} ions near the MOF atoms are plotted after equilibrium is reached.

2. Methodology

MD simulations were performed in the NVT ensemble (constant number of atoms, volume, and temperature) using LAMMPS (Plimpton et al., 2007) v2.0. The Nose-Hoover thermostat was implemented to maintain a temperature of 300 K. In our simulations, periodic boundary conditions were applied in all directions for the whole system. The simulation represents a system where the flexible UiO-66 is placed in the water at t = 0 ns. Initially, the Pb(II) are dispersed in water, away from the MOF. UiO-66 is modelled as a cubic structure with a side length of 20.0 Å. This is placed to the right of the simulation box having the following dimensions: 40.0 Å × 20.0 Å × 20.0 Å, as shown in Fig. 1. Water molecules are dispersed throughout the entire simulation box.

In our work, the source of Pb(II) in water is $Pb(NO_3)_2$, which completely dissociates into Pb^{2+} and NO_3^- ions. These ions are initially inserted in the left side of the simulation box (away from the MOF), as shown in Fig. 1, to create a concentration gradient for diffusion.

The model for the UiO-66 MOF was obtained from X-ray diffraction data file, deposited in the Cambridge Crystallographic Data Centre under code 733458 (Allen and Kennard, 1993). This structure represents the dry form of UiO-66 and is described by Cavka et al. (2008). The bonded force field parameters for the flexible UiO-66 framework representing bond stretching, bond bending and torsions, were obtained from the work of Yang et al. (2011) and are shown in Table S1 in the Supplementary Information. In

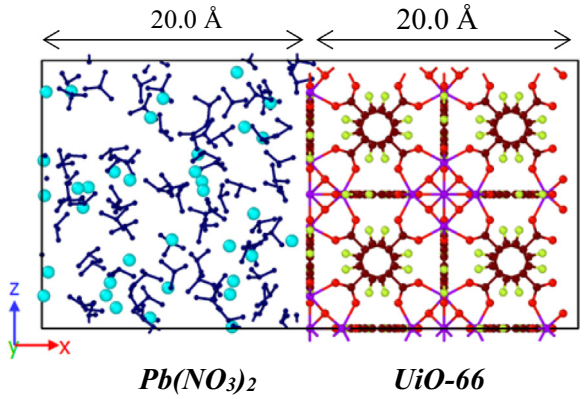

Fig. 1. Snapshot of a simulation system at t = 0 ns, containing 37 Pb^{2+} ions and 74 NO_3^- ions. Color code: Maroon (C in UiO-66), Red (O in UiO-66), Purple (Zr in UiO-66), Green (H in UiO-66), Navy Blue (NO_3^-), and Cyan (Pb^{2+}). Water molecules are not shown in the figure for clarity. (For interpretation of the references to color in this figure legend, the reader is referred to the web version of this article.)

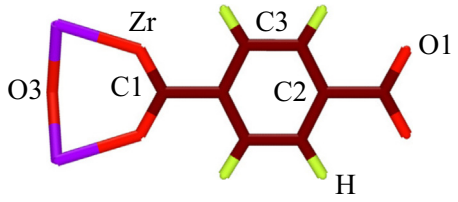

Fig. 2. Labels for the atoms of UiO-66 corresponding to the atomic charges given in Table 1, based on the work of Yang et al., 2011. Color code: Maroon (C in UiO-66), Red (O in UiO-66), Purple (Zr in UiO-66) and Green (H in UiO-66). (For interpretation of the references to color in this figure legend, the reader is referred to the web version of this article.)

Table 1
Non-bonded Interactions Parameters.

Molecule/ion	Atoms	q (e)	σ (Å)	ε (kcal mol^{-1})
UiO-66	C1	0.630	3.473	0.0951
	C2	−0.082		
	C3	−0.065		
	O1	−0.586	3.033	0.0957
	O3	−0.992		
	H	0.133	2.846	0.0152
	Zr	1.968	2.783	0.069
Water	O	−0.830	3.1507	0.1521
	H	0.415	0.4000	0.0460
Pb(II)	Pb^{2+}	2.000	3.000	0.19112
NO_3^-	N	0.950	3.207	0.1600
	O	−0.650	3.349	0.1700

this MOF, metal-oxygen interactions were treated as covalent bonds; bond stretches and bond bending were described by the harmonic potential function and bond torsions were described by the cosine potential function (shown in the Supplementary Information). Interatomic interactions for non-metallic MOF atoms were taken from the DREIDING force field (Mayo et al., 1990). The UFF (Rappé et al., 1992) force field was used to represent interactions of the Zirconium. All the Lennard-Jones interactions were calculated using a cutoff radius of 14 Å. A number of simulation studies showed that these force fields (DREIDING and UFF) can accurately predict the diffusion and adsorption in UiO-66 for various systems (Granato et al., 2014; Nalaparaju and Jiang, 2012; Yang et al., 2011). The partial charges for each atom type in UiO-66 are taken from the DFT calculations by Yang et al. (Yang et al., 2011) with the corresponding atom types shown in Fig. 2. Similar to the work by Kommu et al. (2016), who studied the removal of Pb^{2+} ions (provided by $Pb(NO_3)_2$) from an aqueous solution using graphene sheets: the TIP3P (Jorgensen et al., 1983) model was used to represent non-bonded interactions of water molecules and OPLS-aa (Jorgensen et al., 1996) force field was used for Pb^{2+} and NO_3^- ions. All the force field parameters used in this work are shown in Table 1. Non-bonded interaction parameters for unlike pairs are calculated using Lorentz-Berthelot mixing rules. The latter have been used by previous authors, including the work of Kommu et al. (2016) and Yang et al. (2011) who simulated the aqueous solution and the UiO-66, respectively, using these force fields.

Various cases are simulated in our work to study the effect of changing the cation concentration, the number density of particles and the presence of NO_3^- ions, in a stagnant solution, on the removal of Pb^{2+} ions using UiO-66. These cases are represented in Table 2.

For each case, the corresponding Pb^{2+} and NO_3^- ions are inserted in the left side (x-axis) of the simulation box. Water molecules were dispersed throughout the entire system in all the cases. An energy minimization was performed for each case, to allow the particles to occupy favorable positions within the system. The conjugate gradient minimization algorithm was used and the stopping tolerance for energy and force were 10^{-10} and 10^{-10} kcal/mol-Å, respectively. Consequently, MD simulations were run for 5 ns using a timestep of 0.5 fs. System trajectories were recorded every 5 ps.

To investigate the removal of Pb^{2+} ions using UiO-66, the metal ions are allowed to move freely, with no external force, throughout the simulation box. The concentration of Pb(II) is recorded in two regions of the simulation box: the area containing the MOF and the other area containing only solution with no MOF (referred to as the MOF and empty regions, respectively). These regions are illustrated in Fig. 1.

Additionally, mean square displacements (MSD) were calculated to determine the mobility of the cations for different cases, using Eq. (1).

$$MSD(t) = \frac{1}{N}\sum_{i=1}^{N} |r_i(t+t_0) - r_i(t_0)|^2 \tag{1}$$

where N is the number ions and $r_i(t)$ is the position of ion i at time t.

Radial distribution functions (RDF), $g_{ij}(r)$, for Pb(II) with respect to MOF atoms were also calculated for each case to identify preferential adsorption sites within the MOF, if any. This is given by Eq. (2).

$$g_{ij}(r) = \frac{\Delta N_{ij}(r, r+\Delta r)V}{4\pi r^2 \Delta r N_i N_j} \tag{2}$$

where r is the distance between particles i and j, $\Delta N_{ij}(r, r+\Delta r)$ is the number of particles j around i within a shell from r to $r+\Delta r$, V is the system volume, N_i and N_j are the numbers of species i and j, respectively. In these calculations, particle j corresponds to Pb^{2+} ions.

The adsorption energy, ΔE, between UiO-66 and adsorbate was calculated using Eq. (3), to study the competitive adsorption between Pb^{2+} ions and water molecules on the MOF.

$$\Delta E = E_{UiO-66/A} - (E_{UiO-66} + E_A) \tag{3}$$

where $E_{UiO-66/A}$, E_{UiO-66} and E_A is the potential energy of the adsorbent-adsorbate system, adsorbent (UiO-66 MOF) and adsorbate, respectively.

Table 2
Case studies for stagnant solutions considered in our simulations.

	Number of Pb^{2+} ions	Number of NO_3^- ions	Number of H_2O molecules	Number density of mixture	Metal concentration (M)
Case 1	250	0	250	500	55.6
Case 2	150	0	150	300	55.6
Case 3	37	0	37	74	55.6
Case 4	37	74	37	148	55.6
Case 5	10	0	10	20	55.6
Case 6	10	0	150	160	3.7
Case 7	4	8	37	49	6.0
Case 8	4	8	150	162	1.5
Case 9	10	20	150	180	3.7

3. Results and discussion

First, we observe the effect of changing some system properties in a stagnant solution on Pb^{2+} concentration by viewing snapshots of the system at different stages, studying the number of Pb^{2+} ions in different regions and examining the RDF plots of each system. It should be noted however that the number or percentage uptake of Pb(II) ions reported for each case is only used for comparison between different conditions and is *not* equivalent to the removal of Pb(II) ions from the bulk.

3.1. Effect of the number density of cation/water mixture in the absence of NO_3^- ions

To study the effect of the particles number density within the system on the effectiveness of Pb(II) removal from water using

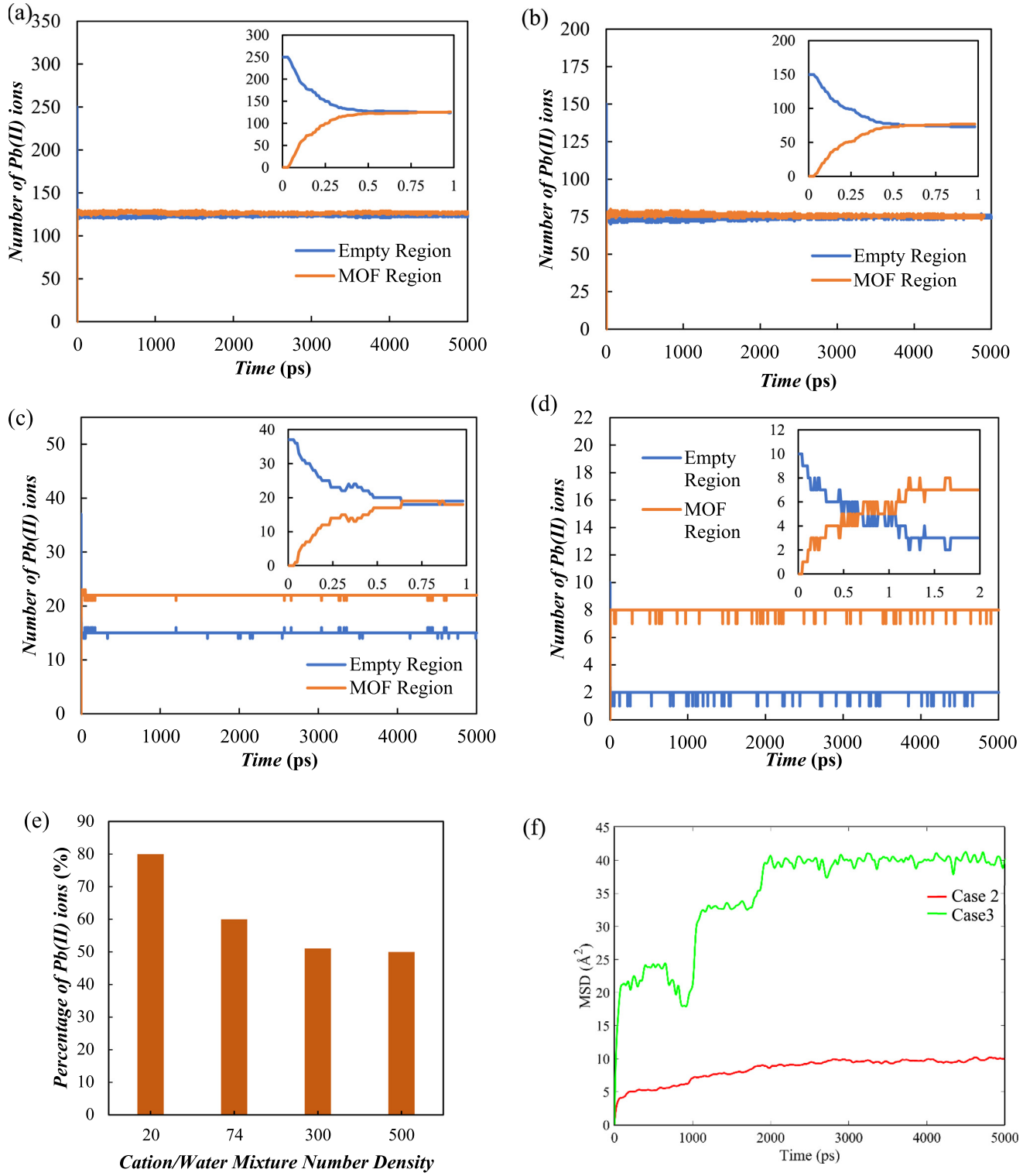

Fig. 3. Concentration of Pb^{2+} ions in the empty and MOF regions for (a) case 1, (b) case 2, (c) case 3 and (d) case 5 corresponding to a cation/water mixture number density of 500, 300, 74 and 20 particles, respectively. Fig. 3(e) shows the percentage of Pb(II) ions adsorbed onto the MOF with respect to the mixture density at equilibrium. Fig. 3(f) is the MSD for Pb^{2+} ions in cases 2 and 3.

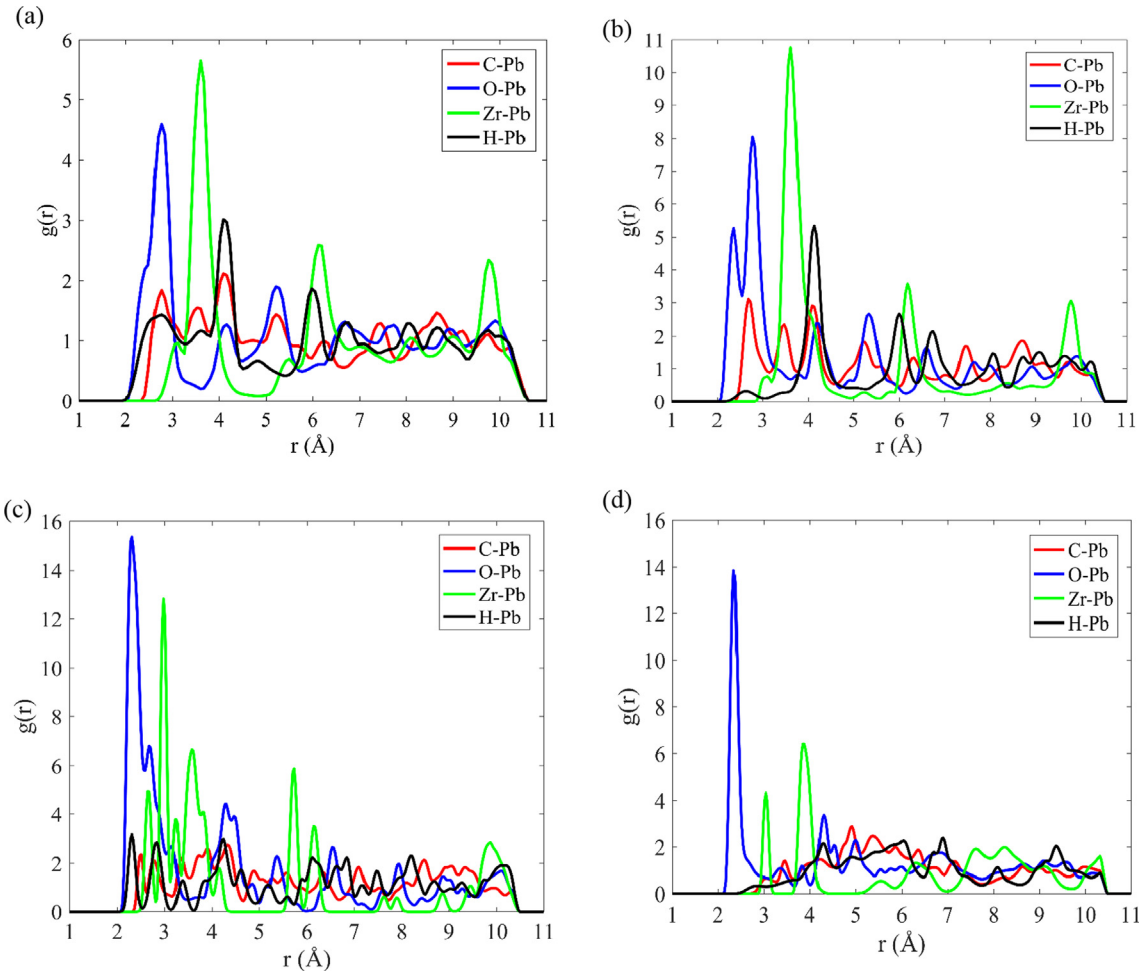

Fig. 4. Radial distribution function of Pb^{2+} ions around the frame work atoms for (a) case 2, (b) case 3, (c) case 5 corresponding to a system number density of 300, 74 and 20 particles, respectively, at a cation concentration of 55.6 M and (d) case 6 corresponding to a cation concentration of 3.7 M.

UiO-66, we compare cases 1, 2, 3, and 5. These contain Pb^{2+} ions and water molecules with a ratio of 1:1 (50% Pb^{2+} and 50% H_2O), with case 1 containing the highest number of 500 particles and case 5 containing the lowest number corresponding to 20 particles. Fig. 3 shows the concentration (expressed in terms of the number of Pb^{2+} ions) for the four cases. It is evident from Fig. 3 that for all the cases, the concentration of Pb^{2+} in the MOF region increases rapidly, in less than 2 ps (as shown by the insets), and is higher than that in the empty region by the end of the simulation time. This indicates that Pb^{2+} ions have the affinity to adsorb onto UiO-66 and not only diffuse due to the concentration gradient. However, the proportion of Pb(II) adsorbed in UiO-66 is higher for systems with lower number density of particles (Fig. 3e). For case 1, 125 out of the 250 (50%) Pb^{2+} ions are in the MOF region by 5 ns, while for cases 2, 3 and 5, 77 out of the 150 (51%), 23 out of the 37 (60%) and 4 out of the 5 (80%) Pb^{2+} ions are in this region, respectively. This decrease in the uptake of Pb^{2+} ions with increasing number density is due to two factors: first, the large number of particles in cases 1 and 2 leads to the obstruction of the diffusing Pb^{2+} ions preventing some ions from entering the MOF region. Ions are freer to diffuse in the less dense systems, cases 3 and 5. Secondly, the MOF contains a fixed number of adsorption sites in all the cases; therefore, once these sites are occupied by metal ions no more Pb^{2+} can be adsorbed. This is validated by the insets in Fig. 3 which show the number of Pb(II) ions in both regions at early stages. The less dense systems take longer to reach equilibrium with more fluctuations evident in the concentration profile. In case 1 for example, the large number of Pb(II) ions (250 ions) means that more ions can enter the MOF region to occupy all the available sites, no extra metal ions can be adsorbed and the system reaches equilibrium faster than other cases with a smaller number of Pb(II) ions (cases 2, 3 and 5). Additionally, fluctuations are due to the smaller number of particles in the system, such as case 5, which lead to more empty space in the simulation box, allowing molecules and ions to diffuse more freely compared to case 2. The lower mobility of metal ions in the denser systems is also supported by the MSD in Fig. 3f which shows that Pb^{2+} ions in case 2, the denser system, have a lower MSD (~10 $Å^2$) than in case 3 (~40 $Å^2$).

It is clear from the RDFs of Pb^{2+} ions around MOF atoms in Fig. 4a, b and c that Pb^{2+} ions are more likely to be packed around the Zr and O atoms, compared to the C and H atoms, in the MOF, indicating the preferential adsorption sites for the metal ions in UiO-66 are near these atoms for the three cases. This shows that electrostatic interactions between Pb^{2+} ions and O atoms is the most probable adsorption mechanism taking place within UiO-66. In UiO-66 there are two types of Zr-O bonds: (1) the Zr–O–Zr bridge found between Zr centers in the cluster and (2) the Zr-O-C link bonding the metal cluster to the BDC linker (oxygen atoms in these linkages are shown as O3 and O1 in Fig. 2, respectively).

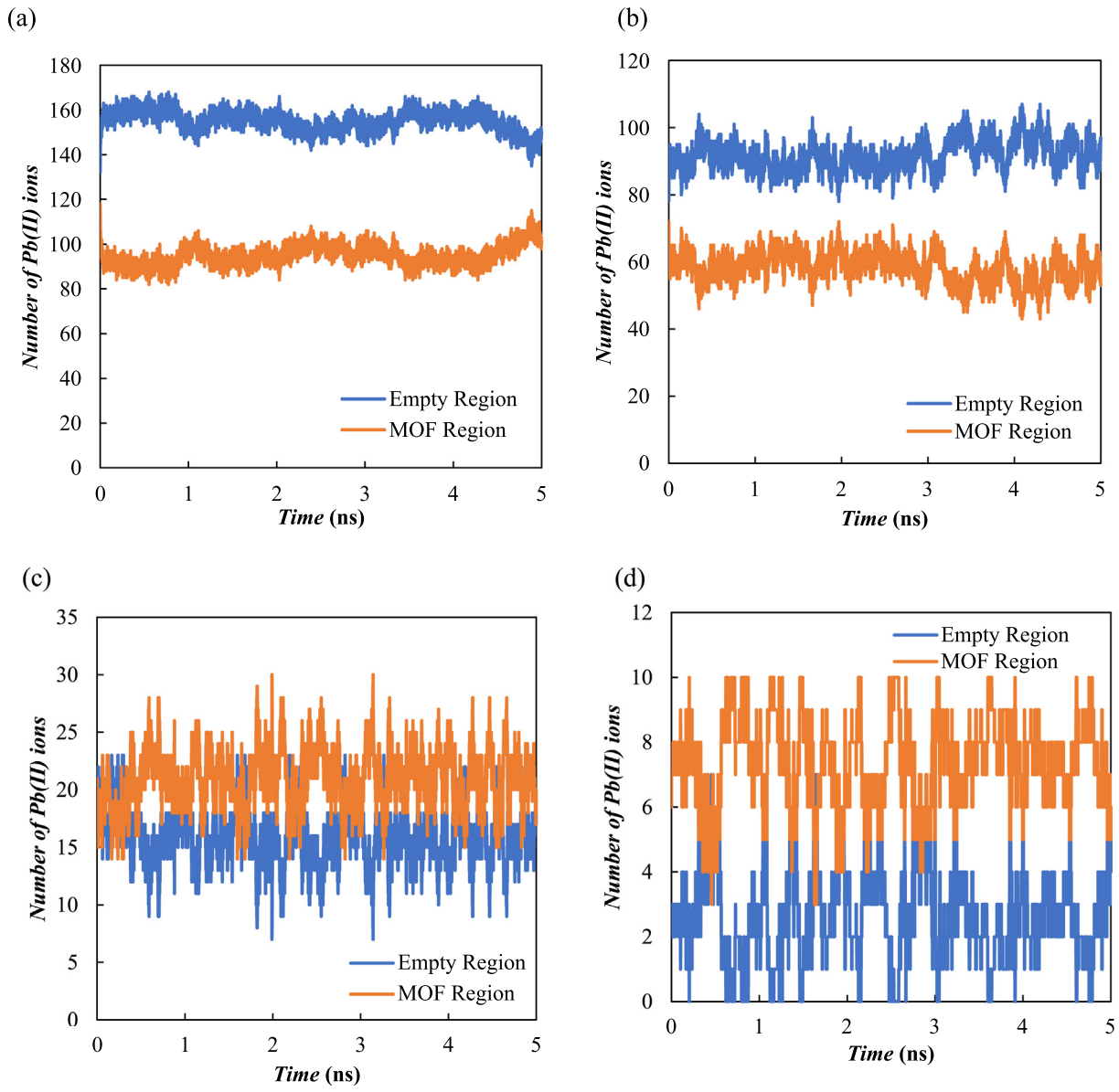

Fig. 5. Concentration of Pb^{2+} ions in the empty and MOF regions for (a) case 1, (b) case 2, (b) case 3 and (c) case 5 corresponding to a cation/water mixture number density of 500, 300, 74 and 20 particles, respectively, in the absence of Coulombic interactions.

Therefore, according to the RDF plots, Pb^{2+} particularly prefer to adsorb near the O atoms forming the Zr–O–Zr bridge, i.e. O3.

Table 1 shows that O3 is more negatively charged than O1, and is the most negatively charged atom in UiO-66, confirming that electrostatic interactions are responsible for this adsorptive removal of Pb(II). These preferential adsorption sites are also evident in the distribution map for the atoms/ions in case 5 at 5 ns, shown in Figure S1 in the Supplementary Information.

Additionally, to further validate the contribution of electrostatic interactions to this adsorption, we switched off the long-range Coulombic interactions in our simulations. As shown by Fig. 5, of all the Pb(II) ions in each case, only 37% (93 out of 250), 38% (57 out of 150), 56% (21 out of 37) and 72% (7.2 out of 10) on average are in the MOF region for cases 1, 2, 3 and 5, respectively. These are 25.4%, 23.6%, 9.1% and 12.5% less ions in the MOF region, respectively, than in the presence of Coulombic interactions (Fig. 3). Additionally, more fluctuations are evident in Fig. 5 indicating that not all the ions in the MOF region are adsorbed but are free to move between the two regions. This supports our hypothesis that electrostatic interactions considerably contribute to the adsorption mechanism of Pb^{2+} ions on UiO-66.

Snapshots of the simulation system for case 3 are shown in Fig. 6. Initially, at t = 0 ns, Pb^{2+} ions reside in solution away from the UiO-66 framework (Fig. 6a). Once the simulation starts, Pb^{2+} ions rapidly diffuse into the MOF region and 59% of the metal ions are in this region by t = 2.5 ns (shown in Fig. 6b). Once in the framework, Pb^{2+} ions prefer being adsorbed without leaving the MOF region. This is evident in Fig. 6c which shows that the same Pb^{2+} ions (with the same particle IDs as those in Fig. 6b) are adsorbed at the same sites in UiO-66 by t = 5 ns. It should be noted that, after investigating the individual particle trajectories of the Pb^{2+} ions, all the metal cations in the MOF region are adsorbed and are not only in dynamic equilibrium, making the process strictly one-directional.

Therefore, the number of metal ions in the MOF region is equivalent to the number of ions adsorbed in UiO-66. Simulations of cases 1, 2, 5 and 6 (containing no NO_3^- ions) exhibit a similar process to that shown in Fig. 6.

In water-mediated systems, such as the ones simulated, water molecules are expected to adsorb on the UiO-66 framework forming hydrogen bonds with the oxygen atoms in the MOF (Phang et al., 2015). However, Fig. 7 shows that the adsorption energy of one Pb^{2+} ion on UiO-66 is −3610 kJ/mol which is less than that of one water molecule adsorbing on the MOF (−343 kJ/mol). This indicates that Pb^{2+} has a stronger interaction with the framework and adsorbs more strongly than water. The more negative value in Fig. 7 shows that the Pb^{2+} adsorption on UiO-66 is thermodynamically more favorable than that of water molecules, probably due to the positive charge of this metal ion. A similar result was obtained for the adsorption of more Pb(II) ions on UiO-66 (shown in Figure S1 in the Supplementary Information). Therefore, from an energy point of view, water molecules do not compete with Pb^{2+} ions for adsorption sites on UiO-66.

3.2. Effect of cation concentration in the absence of NO_3^- ions

The solutions represented by cases 5 and 6 contain a Pb(II) concentration corresponding to 55.6 M and 3.7 M, respectively. These Pb(II) concentrations are significantly higher than those found in drinking water, which is less than 2.42×10^{-8} M in the US (US Department of Health and Human Services, 2016) for example. But these case studies represent the high concentration of the metal found in the vicinity of the MOF in solution. A comparison of Pb^{2+} concentration in the empty and MOF regions for these two cases is shown in Fig. 8.

The Pb^{2+} concentration is higher in the MOF region than the empty one, for both cases, indicating the successful removal of these metal ions using UiO-66. However, the solution containing 55.6 M of Pb(II) (case 5) resulted in a higher removal of Pb^{2+} ions of 80% compared to 60% for case 6, by 5 ns (Fig. 8c). In the less concentrated solution, Pb(II) ions are surrounded by more water molecules. These hinder the diffusion of Pb(II) towards the MOF in case 6, leading to a lower uptake of the metal. As mentioned previously, less dense systems show more fluctuations in the concentration profile of Pb(II) ions, take longer to reach equilibrium but eventually lead to a higher uptake of Pb(II) ions by the MOF. The RDFs for Pb(II) around UiO-66 atoms shown in Fig. 4c and d, for cases 5 and 6, respectively, indicate that Pb^{2+} ions preferentially adsorb onto the O atoms in UiO-66, as discussed previously in section 3.1.

3.3. Effect of the presence of NO_3^- ions

Nitrate ions in the vicinity of the MOF will affect Pb(II) removal using UiO-66 due to the intermolecular forces between the Pb^{2+} and NO_3^- ions. This is studied by comparing Pb^{2+} concentration in the empty and MOF regions for cases 3 and 4, corresponding to a cation concentration of 55.6 M, as shown in Fig. 9.

The presence of NO_3^- ions in the system leads to a 95% decrease in Pb(II) removal, leaving almost all the metal ions in the empty region of the simulation box. This is due to the intermolecular interaction between the cation (Pb^{2+}) and the anion (NO_3^-), which is stronger than that between UiO-66 and Pb^{2+} ions. This strong interaction is also evident in Fig. 10 which shows that in the presence of NO_3^- ions, case 4, very few Pb^{2+} ions (orange) are in the MOF region and are closely positioned to the anions (red and maroon) in the empty region. Hence, an external force may be required to facilitate the interaction between the metal ions and UiO-66, leading to their removal.

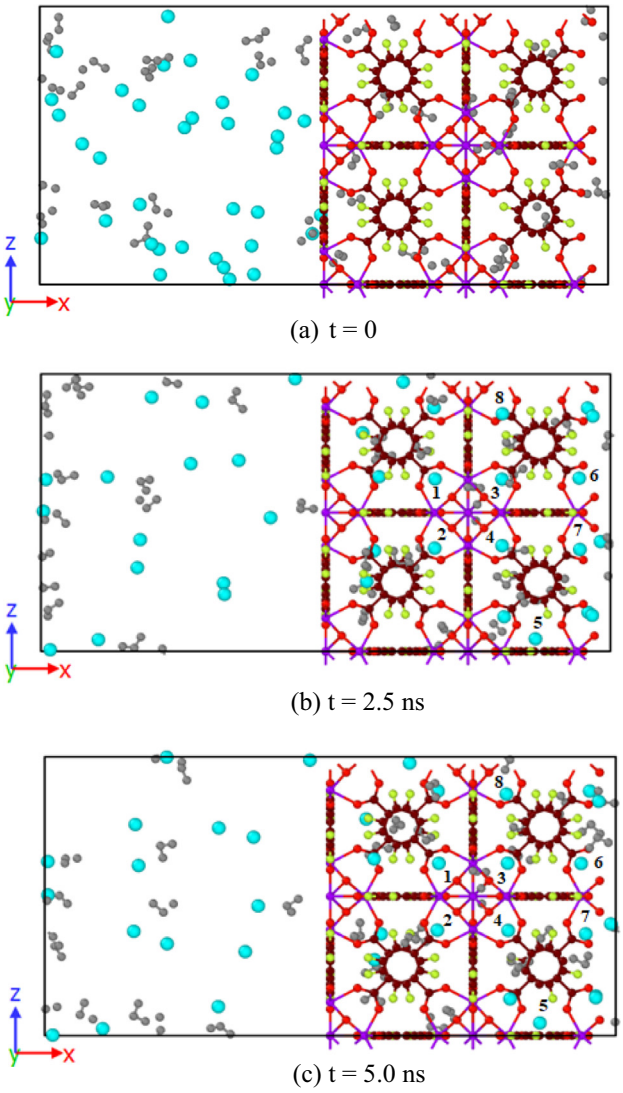

Fig. 6. Snapshots of the simulation system for case 3 at: (a) t = 0 ns, (b) t = 2.5 ns and (c) t = 5.0 ns. Color code: Maroon (C in UiO-66), Red (O in UiO-66), Purple (Zr in UiO-66), Green (H in UiO-66), Gray (NO_3^-), and Cyan (Pb_2^+). Labels 1 to 8 indicate the particle ID of some Pb_2^+ ions in the MOF region. (For interpretation of the references to color in this figure legend, the reader is referred to the web version of this article.)

3.4. Effect of cation concentration in the presence of NO_3^- ions

The solutions represented by cases 7, 8 and 9 contain NO_3^- ions and a Pb(II) concentration corresponding to 6 M, 1.5 M and 3.7 M, respectively. As mentioned earlier, these Pb(II) concentrations are significantly higher than those found in drinking water and represent the high concentration of the metal found near the MOF in solution. Fig. 11 shows a comparison of Pb^{2+} ions concentration in the empty and MOF regions for cases 7, 8 and 9.

As expected from the previous section, the presence of NO_3^- ions causes most of the Pb^{2+} ions to remain in the empty region for all the cases in Fig. 11. Changing the metal cation concentration led to no change in the observed behavior with 75%, 75% and 70% of Pb(II) remaining in the empty region for cases 7, 8 and 9, respectively

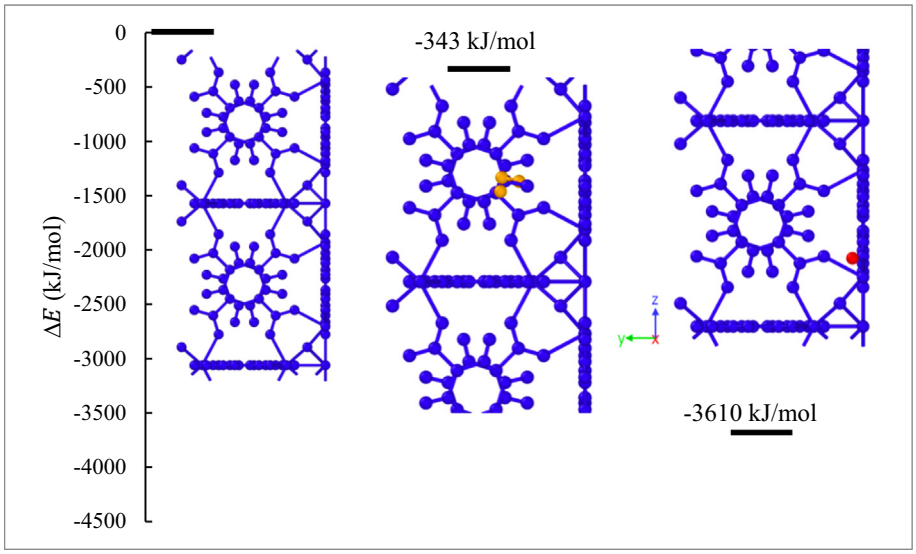

Fig. 7. Energy-level diagram of the adsorption of Pb(II) ions and water molecules on UiO-66. The adsorption energy of one water molecule (orange) on the framework (blue) is −343 kJ/mol and that of one Pb(II) ion (red) on the MOF is −3610 kJ/mol. (For interpretation of the references to color in this figure legend, the reader is referred to the web version of this article.)

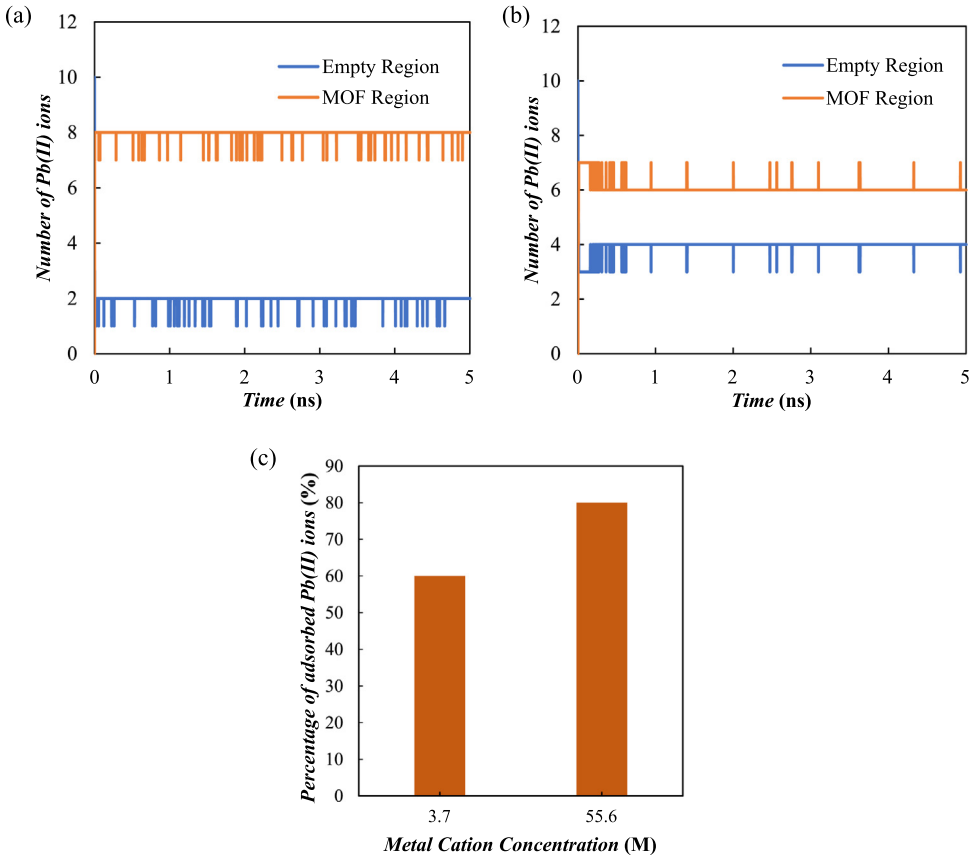

Fig. 8. Concentration of Pb^{2+} ions in the empty and MOF regions for (a) case 5 and (b) case 6 corresponding to a cation concentration of 55 M and 3.7 M, respectively. Fig. 8(c) shows the percentage of Pb(II) ions adsorbed with respect to the cation concentration in the system at equilibrium.

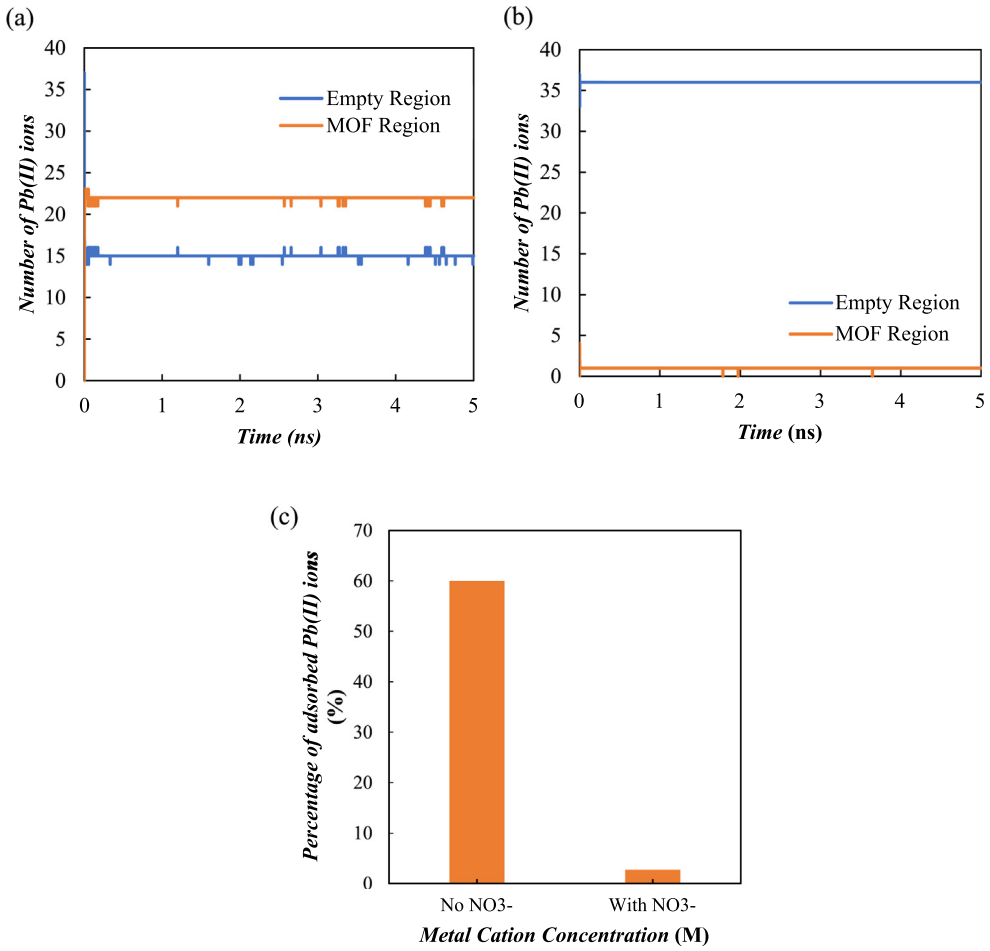

Fig. 9. Concentration of Pb^{2+} ions in the empty and MOF regions for (a) case 3 and (b) case 4 in the absence and presence of nitrate ions, respectively. Fig. 8(c) shows the percentage of Pb(II) ions adsorbed for the two cases after equilibrium is reached.

(Fig. 11d). The distribution maps for these three cases are shown in Figure S1 in the Supplementary Information.

4. Conclusions

We studied the removal of Pb^{2+} ions using UiO-66 using molecular dynamics simulations. The results for stagnant solutions suggest that this removal is probably successful under favorable conditions. The optimal conditions for Pb^{2+} removal using UiO-66 are: low number density of particles in the system, high metal concentration and absence of NO_3^- ions in the vicinity of the MOF. The large number of particles surrounding Pb(II) in a high number density system hinder the metal ions' diffusion towards the MOF leading to a lower uptake. The high metal concentration in these simulations is representative of a large number of Pb^{2+} ions near the MOF in solution.

The proposed adsorption mechanism taking place is electrostatic interaction between the oxygen atoms in the Zr–O–Zr bridge and Pb(II). This is facilitated by the oxygen atom having the most negative charge in UiO-66. Also, the Pb^{2+} ions' adsorption on UiO-66 is thermodynamically more favorable than that of water molecules so that the metal ions can occupy these sites without competition from water molecules.

Additionally, NO_3^- ions near the MOF lead to a reduced uptake of Pb^{2+} ions by UiO-66 regardless of the metal concentration. However, the number of NO_3^- ions around the MOF cannot be experimentally controlled for a stagnant solution. Future work could investigate the addition of an external force to facilitate the

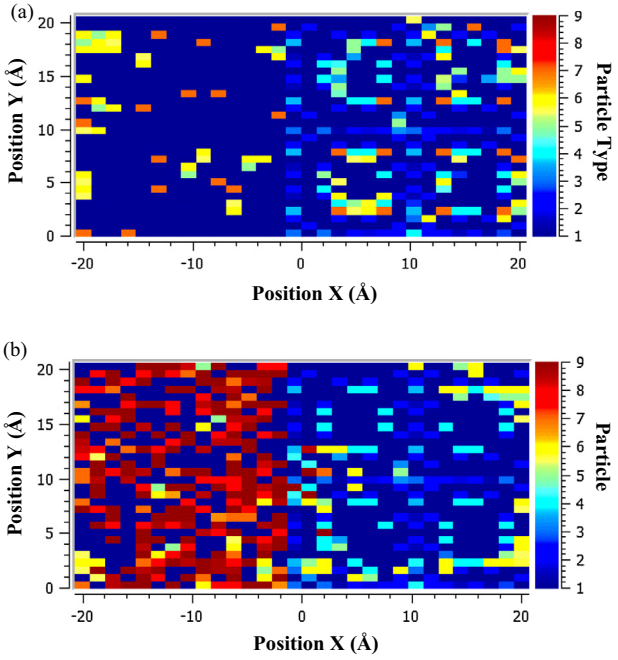

Fig. 10. Distribution map of the atoms/ions in (a) case 3 (no NO_3^-) and (b) case 4 (with NO_3^-), at 5 ns. The color bar indicates the color corresponding to each 'particle type'. The nine 'particle types' in the system are: 1 – Carbon (UiO-66), 2 – Oxygen (UiO-66), 3 – Zirconium (UiO-66), 4 – Hydrogen (UiO-66), 5 – Oxygen (water), 6 – Hydrogen (water), 7 – Lead ion, 8 – Nitrogen (NO_3^-) and 9 – Oxygen (NO_3^-).

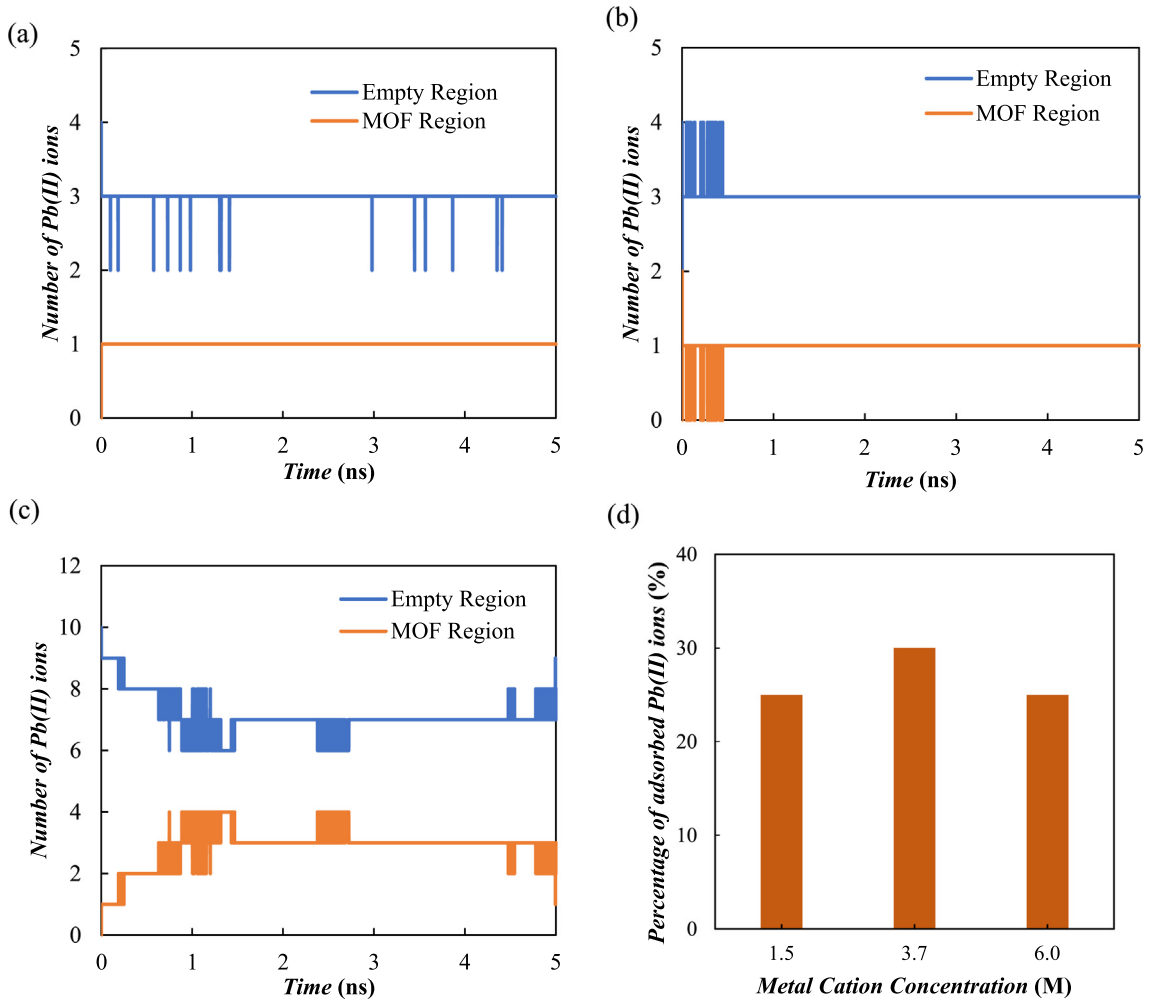

Fig. 11. Concentration of Pb^{2+} ions in the empty and MOF regions for (a) case 7, (b) case 8 and (c) case 9 corresponding to a cation concentration of 6 M, 1.5 M and 3.7 M, respectively. Fig. 11(d) shows the percentage of Pb(II) ions adsorbed on the MOF as a function of metal cation concentration for these cases.

removal of Pb^{2+} ions by UiO-66 in the presence these anions. Even though these results require experimental validation, they indicate that UiO-66 can successfully remove Pb(II) from water and provide insightful information on the mechanism taking place.

Declaration of Competing Interest

The authors declare that they have no known competing financial interests or personal relationships that could have appeared to influence the work reported in this paper.

Acknowledgments

Support from the Research Board at the American University of Beirut is greatly acknowledged. This research did not receive any specific grant from funding agencies in the public, commercial, or not-for-profit sectors.

Appendix A. Supplementary material

Supplementary data to this article can be found online at https://doi.org/10.1016/j.ces.2019.115396.

References

Agency for Toxic Substances and Disease Registry, 2007. Toxicological Profile for Lead. Atlanta.

Allen, F.H., Kennard, O., 1993. 3D search and research using the Cambridge structural database. Chem. Des. Autom. News 8, 31–37.

Barakat, M.A., 2011. New trends in removing heavy metals from industrial wastewater. Arab. J. Chem. 4, 361–377. https://doi.org/10.1016/J.ARABJC.2010.07.019.

Bradl, H., 2005. Heavy Metals in the Environment: [origin, interaction and remediation]. Elsevier Academic Press.

Burrows, A.D., Cassar, K., Düren, T., Friend, R.M.W., Mahon, M.F., Rigby, S.P., Savarese, T.L., 2008. Syntheses, structures and properties of cadmium benzenedicarboxylate metal–organic frameworks. Dalt. Trans., 2465 https://doi.org/10.1039/b718947h.

Cavka, J.H., Olsbye, U., Guillou, N., Bordiga, S., Lillerud, K.P., 2008. A New zirconium inorganic building brick forming metal organic frameworks with exceptional stability – Supp. Info. J. Am. Chem. Soc. 6, 1–19. https://doi.org/10.1021/ja8057953.

Custelcean, R., Sellin, V., Moyer, B.A., 2007. Sulfate separation by selective crystallization of a urea-functionalized metal–organic framework. Chem. Commun., 1541–1543 https://doi.org/10.1039/B616761F.

Cychosz, K.A., Matzger, A.J., 2010. Water stability of microporous coordination polymers and the adsorption of pharmaceuticals from water. Langmuir 26, 17198–17202. https://doi.org/10.1021/la103234u.

DeCoste, J.B., Peterson, G.W., Schindler, B.J., Killops, K.L., Browe, M.A., Mahle, J.J., 2013. The effect of water adsorption on the structure of the carboxylate containing metal–organic frameworks Cu-BTC, Mg-MOF-74, and UiO-66. J. Mater. Chem. A 1, 11922. https://doi.org/10.1039/c3ta12497e.

Dietzel, P.D.C., Johnsen, R.E., Fjellvåg, H., Bordiga, S., Groppo, E., Chavan, S., Blom, R., 2008. Adsorption properties and structure of CO2 adsorbed on open coordination sites of metal–organic framework Ni2(dhtp) from gas adsorption, IR spectroscopy and X-ray diffraction. Chem. Commun. 5125–27. https://doi.org/10.1039/b810574j.

Dincă, M., Long, J.R., 2008. Hydrogen storage in microporous metal-organic frameworks with exposed metal sites. Angew. Chemie Int. Ed. 47, 6766–6779. https://doi.org/10.1002/anie.200801163.

Duffus, J.H., 2002. "Heavy Metals"—a meaningless term?. Pure Appl. Chem. 74, 793–807.

Environmental Protection Agency, 2019. Basic Information about Lead in Drinking Water [WWW Document]. URL <https://www.epa.gov/ground-water-and-

drinking-water/basic-information-about-lead-drinking-water#regs> (accessed 4.18.18).
Farrusseng, D., Aguado, S., Pinel, C., 2009. Metal-organic frameworks: opportunities for catalysis. Angew. Chemie Int. Ed. 48, 7502–7513. https://doi.org/10.1002/anie.200806063.
Flora, G., Gupta, D., Tiwari, A., 2012. Toxicity of lead: a review with recent updates. Interdiscip. Toxicol. 5, 47–58. https://doi.org/10.2478/v10102-012-0009-2.
Fu, F., Wang, Q., 2011. Removal of heavy metal ions from wastewaters: a review. J. Environ. Manage. 92, 407–418. https://doi.org/10.1016/j.jenvman.2010.11.011.
Granato, M.A., Martins, V.D., Ferreira, A.F.P., Rodrigues, A.E., 2014. Adsorption of xylene isomers in MOF UiO-66 by molecular simulation. Microporous Mesoporous Mater. 190, 165–170. https://doi.org/10.1016/j.micromeso.2014.02.014.
Greathouse, J.A., Allendorf, M.D., 2006. The interaction of water with MOF-5 simulated by molecular dynamics. J. Am. Chem. Soc. 128, 10678–10679. https://doi.org/10.1021/ja063506b.
Halder, G.J., Kepert, C.J., Moubaraki, B., Murray, K.S., Cashion, J.D., 2002. Guest-dependent spin crossover in a nanoporous molecular framework material. Science (80-.) 298, 1762–1765. https://doi.org/10.1126/science.1075948.
Harvey, B., 2002. Managing Elevated Blood Lead Levels Among Young Children: Recommendations from the Advisory Committee on Childhood Lead Poisoning Prevention. Atlanta.
Hasan, Z., Jhung, S.H., 2015. Removal of hazardous organics from water using metal-organic frameworks (MOFs): plausible mechanisms for selective adsorptions. J. Hazard. Mater. 283, 329–339.
Horcajada, P., Serre, C., Vallet-Regí, M., Sebban, M., Taulelle, F., Férey, G., 2006. Metal-organic frameworks as efficient materials for drug delivery. Angew. Chemie Int. Ed. 45, 5974–5978. https://doi.org/10.1002/anie.200601878.
Howarth, A.J., Katz, M.J., Wang, T.C., Platero-Prats, A.E., Chapman, K.W., Hupp, J.T., Farha, O.K., 2015. High efficiency adsorption and removal of selenate and selenite from water using metal-organic frameworks. J. Am. Chem. Soc. 137, 7488–7494. https://doi.org/10.1021/jacs.5b03904.
Ihsanullah, Abbas A., Al-Amer, A.M., Laoui, T., Al-Marri, M.J., Nasser, M.S., Khraisheh, M., Atieh, M.A., 2016. Heavy metal removal from aqueous solution by advanced carbon nanotubes: critical review of adsorption applications. Sep. Purif. Technol. 157, 141–161. https://doi.org/10.1016/j.seppur.2015.11.039.
Jamali, A., Tehrani, A.A., Shemirani, F., Morsali, A., 2016. Lanthanide metal–organic frameworks as selective microporous materials for adsorption of heavy metal ions. Dalt. Trans. 45, 9193–9200. https://doi.org/10.1039/C6DT00782A.
Jorgensen, W.L., Chandrasekhar, J., Madura, J.D., Impey, R.W., Klein, M.L., 1983. Comparison of simple potential functions for simulating liquid water. J. Chem. Phys. 79, 926–935. https://doi.org/10.1063/1.445869.
Jorgensen, W.L., Maxwell, D.S., Tiradorives, J., 1996. Development and testing of the OPLS all atom force field on conformational energetics and properties of organic liquids. J. Am. Chem. Soc. https://doi.org/10.1021/ja9621760.
Ke, F., Qiu, L.-G., Yuan, Y.-P., Peng, F.-M., Jiang, X., Xie, A.-J., Shen, Y.-H., Zhu, J.-F., 2011. Thiol-functionalization of metal-organic framework by a facile coordination-based postsynthetic strategy and enhanced removal of Hg_2^+ from water. J. Hazard. Mater. 196, 36–43. https://doi.org/10.1016/j.jhazmat.2011.08.069.
Khan, N.A., Jung, B.K., Hasan, Z., Jhung, S.H., 2015. Adsorption and removal of phthalic acid and diethyl phthalate from water with zeolitic imidazolate and metal–organic frameworks. J. Hazard. Mater. 282, 194–200. https://doi.org/10.1016/J.JHAZMAT.2014.03.047.
Kommu, A., Namsani, S., Singh, J.K., 2016. Removal of heavy metal ions using functionalized graphene membranes: a molecular dynamics study. RSC Adv. 6, 63190–63199. https://doi.org/10.1039/C6RA06817K.
Lee, J., Farha, O.K., Roberts, J., Scheidt, K.A., Nguyen, S.T., Hupp, J.T., 2009. Metal–organic framework materials as catalysts. Chem. Soc. Rev. 38, 1450. https://doi.org/10.1039/b807080f.
Li, C.-J., Lin, Z., Peng, M.-X., Leng, J.-D., Yang, M.-M., Tong, M.-L., 2008a. Novel three-dimensional 3d–4f microporous magnets exhibiting selective gas adsorption behavior. Chem. Commun., 6348 https://doi.org/10.1039/b815024a.
Li, K., Lee, J., Olson, D.H., Emge, T.J., Bi, W., Eibling, M.J., Li, J., 2008b. Unique gas and hydrocarbon adsorption in a highly porous metal-organic framework made of extended aliphatic ligands. Chem. Commun. 6123. https://doi.org/10.1039/b814498b.
Lin, K.Y.A., Liu, Y.T., Chen, S.Y., 2016. Adsorption of fluoride to UiO-66-NH2 in water: Stability, kinetic, isotherm and thermodynamic studies. J. Colloid Interface Sci. 461, 79–87. https://doi.org/10.1016/j.jcis.2015.08.061.
Liu, X., Demir, N.K., Wu, Z., Li, K., 2015. Highly water-stable zirconium metal-organic framework UiO-66 membranes supported on alumina hollow fibers for desalination. J. Am. Chem. Soc. 137, 6999–7002. https://doi.org/10.1021/jacs.5b02276.
Luo, X., Ding, L., Luo, J., 2015. Adsorptive removal of Pb(II) ions from aqueous samples with amino-functionalization of metal-organic frameworks MIL-101 (Cr). J. Chem. Eng. Data 60, 1732–1743. https://doi.org/10.1021/je501115m.
Mayo, L., Olafson, D., Goddard, W.A., 1990. DREIDING: a generic force field for molecular simulations. J. Phys. Chem. 94, 8897.
Murray, L.J., Dincă, M., Long, J.R., 2009. Hydrogen storage in metal–organic frameworks. Chem. Soc. Rev. 38, 1294. https://doi.org/10.1039/b802256a.
Nalaparaju, A., Jiang, J., 2012. Ion exchange in metal-organic framework for water purification: insight from molecular simulation. J. Phys. Chem. C 116, 6925–6931. https://doi.org/10.1021/jp210082f.
Phang, W.J., Jo, H., Lee, W.R., Song, J.H., Yoo, K., Kim, B., Hong, C.S., 2015. Superprotonic conductivity of a UiO-66 framework functionalized with sulfonic acid groups by facile postsynthetic oxidation. Angew. Chemie Int. Ed. 54, 5142–5146. https://doi.org/10.1002/anie.201411703.
Plimpton, S., Crozier, P., Thompson, A., 2007. LAMMPS-large-scale atomic/molecular massively parallel simulator. Sandia Natl. Lab. 18, 43.
Qin, Q., Wang, Q., Fu, D., Ma, J., 2011. An efficient approach for Pb(II) and Cd(II) removal using manganese dioxide formed in situ. Chem. Eng. J. 172, 68–74. https://doi.org/10.1016/J.CEJ.2011.05.066.
Rappé, A.K., Casewit, C.J., Colwell, K.S., Goddard, W.A., Skiff, W.M., 1992. UFF, a full periodic table force field for molecular mechanics and molecular dynamics simulations. J. Am. Chem. Soc. 114, 10024–10035. https://doi.org/10.1021/ja00051a040.
Seo, Y.S., Khan, N.A., Jhung, S.H., 2015. Adsorptive removal of methylchlorophenoxypropionic acid from water with a metal-organic framework. Chem. Eng. J. 270, 22–27. https://doi.org/10.1016/J.CEJ.2015.02.007.
Tahmasebi, E., Masoomi, M.Y., Yamini, Y., Morsali, A., 2015. Application of mechanosynthesized azine-decorated Zinc(II) metal-organic frameworks for highly efficient removal and extraction of some heavy-metal ions from aqueous samples: a comparative study. Inorg. Chem. 54, 425–433. https://doi.org/10.1021/ic5015384.
Tchounwou, P.B., Yedjou, C.G., Patlolla, A.K., Sutton, D.J., 2012. Heavy Metal Toxicity and the Environment, in: Molecular, Clinical and Environmental Toxicology. Springer, Basel, pp. 133–164. Doi: 10.1007/978-3-7643-8340-4_6.
US Department of Health and Human Services, 2016. Lead and Lead Compounds, 14th Report on Carcinogens.
Vu, T.A., Le, G.H., Dao, C.D., Dang, L.Q., Nguyen, K.T., Nguyen, Q.K., Dang, P.T., Tran, H. T.K., Duong, Q.T., Nguyen, T.V., Lee, G.D., 2015. Arsenic removal from aqueous solutions by adsorption using novel MIL-53(Fe) as a highly efficient adsorbent. RSC Adv. 5, 5261–5268. https://doi.org/10.1039/C4RA12326C.
Wang, C., Liu, X., Chen, J.P., Li, K., 2015. Superior removal of arsenic from water with zirconium metal-organic framework UiO-66. Sci. Rep. 5, 1–10. https://doi.org/10.1038/srep16613.
Wang, K., Gu, J., Yin, N., 2017a. Efficient removal of Pb(II) and Cd(II) using NH2-functionalized Zr-MOFs via rapid microwave-promoted synthesis. Ind. Eng. Chem. Res. 56, 1880–1887. https://doi.org/10.1021/acs.iecr.6b04997.
Wang, L., Zhao, X., Zhang, J., Xiong, Z., 2017b. Selective adsorption of Pb (II) over the zinc-based MOFs in aqueous solution-kinetics, isotherms, and the ion exchange mechanism. Environ. Sci. Pollut. Res. 24, 14198–14206. https://doi.org/10.1007/s11356-017-9002-9.
WHO, 2008. International Health Regulations, 2nd ed. Geneva.
Yang, Q., Jobic, H., Salles, F., Kolokolov, D., Guillerm, V., Serre, C., Maurin, G., 2011. Probing the dynamics of CO_2 and CH_4 within the porous zirconium terephthalate UiO-66(Zr): a synergic combination of neutron scattering measurements and molecular simulations. Chem. – A Eur. J. 17, 8882–8889. https://doi.org/10.1002/chem.201003596.
Yee, K.-K., Reimer, N., Liu, J., Cheng, S.-Y., Yiu, S.-M., Weber, J., Stock, N., Xu, Z., 2013. Effective mercury sorption by thiol-laced metal-organic frameworks: in strong acid and the vapor phase. J. Am. Chem. Soc. 135, 7795–7798. https://doi.org/10.1021/ja400212k.
Yin, N., Wang, K., Li, Z., 2016. Rapid microwave-promoted synthesis of Zr-MOFs: an efficient adsorbent for Pb(II) removal. Chem. Lett. 45, 625–627. https://doi.org/10.1246/cl.160148.
Zhang, J., Xiong, Z., Li, C., Wu, C., 2016. Exploring a thiol-functionalized MOF for elimination of lead and cadmium from aqueous solution. J. Mol. Liq. 221, 43–50. https://doi.org/10.1016/J.MOLLIQ.2016.05.054.
Zhou, H.C., Long, J.R., Yaghi, O.M., 2012. Introduction to metal-organic frameworks. Chem. Rev. 112, 673–674. https://doi.org/10.1021/cr300014x.
Zou, F., Yu, R., Li, R., Li, W., 2013. Microwave-assisted synthesis of HKUST-1 and functionalized HKUST-1-MW@H3PW12O40: selective adsorption of heavy metal ions in water analyzed with synchrotron radiation. ChemPhysChem 14, 2825–2832. https://doi.org/10.1002/cphc.201300215.